

Atomistic Simulation of Nafion Membrane. 2. Dynamics of Water Molecules and Hydronium Ions

R. Devanathan,* A. Venkatnathan, and M. Dupuis

Fundamental Science Directorate, Pacific Northwest National Laboratory, Richland, Washington 99352

Received: July 31, 2007; In Final Form: September 10, 2007

We have performed a detailed and comprehensive analysis of the dynamics of water molecules and hydronium ions in hydrated Nafion using classical molecular dynamics simulations with the DREIDING force field. In addition to calculating diffusion coefficients as a function of hydration level, we have also determined mean residence time of H₂O molecules and H₃O⁺ ions in the first solvation shell of SO₃[−] groups. The diffusion coefficient of H₂O molecules increases with increasing hydration level and is in good agreement with experiment. The mean residence time of H₂O molecules decreases with increasing membrane hydration from 1 ns at a low hydration level to 75 ps at the highest hydration level studied. These dynamical changes are related to the changes in membrane nanostructure reported in the first part of this work. Our results provide insights into slow proton dynamics observed in neutron scattering experiments and are consistent with the Gebel model of Nafion structure.

1. Introduction

Polymer electrolyte membrane (PEM) fuel cells convert chemical energy to electrical energy with high efficiency and minimal pollution. Their widespread deployment as part of the proposed hydrogen economy¹ can reduce dependence on fossil fuels, environmental pollution, and greenhouse gas emissions. Currently, PEM fuel cells use perfluorosulfonic acid (PFSA)-based membranes, such as Nafion developed by DuPont. The desired membrane properties for this application include high proton conductivity at low hydration levels, thermal, mechanical, and chemical stability, durability under prolonged operation, and low cost. None of the existing membranes meet all the requirements and there is a pressing need to develop novel membranes based on a molecular level understanding of membrane chemistry and nanostructure.

In PFSA membranes, water molecules play a multifaceted role as a shuttle for proton transport, reaction product, coolant, and an impediment to reactant transport at high concentrations.² The dynamics of water molecules confined within nanoscale regions of PFSA membranes, especially at low hydration levels, is remarkably different from that of water molecules in bulk water.³ A fundamental understanding of the relationship between membrane nanostructure and the dynamics of water molecules is needed for the development of efficient, reliable, and cost-effective membranes to advance PEM fuel cell technology.

In an effort to interpret experimental data and understand the relationship between Nafion membrane nanostructure and molecular transport, we have performed classical molecular dynamics (MD) simulations using an all-atom force field at levels of membrane hydration chosen to match experiment.^{4–7} We use the term nanostructure to refer to the structure within the water pores and channels in Nafion membrane. In the first part of our work,⁸ we examined the effect of hydration on membrane nanostructure and showed that water molecules and hydronium ions are strongly bound to sulfonate groups for λ

less than 7. We showed that multiple sulfonate groups surround the hydronium ion at low hydration.^{8,9} In the present report, we compute the dynamical properties of water molecules and hydronium ions in Nafion and relate them to the structural changes reported previously.⁸

Proton and small molecule transport in Nafion membrane has been extensively studied by experiment. Kreuer et al.¹⁰ have reviewed transport in proton conductors for fuel cell applications. They have highlighted the differences in transport mechanisms with changes in the level of hydration, which is the ratio of water molecules per sulfonic acid group in Nafion and is typically represented by λ . Kreuer et al.¹⁰ have stated that the mechanism of proton conduction is structural diffusion at high levels of hydration ($\lambda > 10$) and vehicular transport (H₃O⁺) at intermediate and low levels of hydration. In this report, the terms structural diffusion and structural transport of protons are used to refer to the Grotthuss mechanism that has been discussed in great detail by Marx et al.¹¹

Zawodzinski et al.⁴ determined proton diffusion coefficients from conductivity measurements and water diffusion coefficients from nuclear magnetic resonance (NMR) measurements in Nafion at various levels of hydration (λ ranging from 2 to 22). The two diffusion coefficients are comparable at low λ (~ 3), while the proton diffusion coefficient diverges to higher values as λ increases. The authors have inferred from these results that structural diffusion becomes more significant at higher λ due to more bulklike behavior of water, which is consistent with the conclusions of Kreuer et al.¹⁰

Pivovar and Pivovar⁵ examined hydrated Nafion 117 using quasi-elastic neutron scattering (QENS) and observed two distinct regimes of dynamical behavior. The notation 117 refers to equivalent weight of 1100 g/mol of SO₃[−] group and a membrane thickness of 0.007 in. Pivovar and Pivovar⁵ fitted their data using two different models based on continuous diffusion within a sphere and unconstrained random diffusion and extracted water residence times of the order of 10 ps. The diffusion coefficients of water molecules obtained by Pivovar

* Corresponding author. Email: ram.devanathan@pnl.gov.

and Pivovar⁵ using QENS are considerably greater than those reported by Zawodzinski et al.⁴ using the NMR technique.

The water molecule residence time reported by Pivovar and Pivovar⁵ decreases rapidly with increasing λ up to $\lambda = 6$ and then levels off, indicating increasing water mobility with increasing λ . This is consistent with an infrared spectroscopy study⁶ that reported an abrupt structural change in hydrated Nafion around $\lambda = 5$. The simulation results discussed in the first part of this work⁸ provide an explanation for this structural change in terms of coordination of hydronium ions by multiple sulfonate groups.

In contrast to the work of Pivovar and Pivovar,⁵ a recent QENS study⁷ of water dynamics in hydrated Nafion 112 has used a single theoretical model based on Gaussian statistics valid over the whole neutron momentum transfer (Q) range to fit the data. This recent study⁷ has concluded that there are two distinct populations of diffusing proton. Both have characteristic length scales of 2–4 Å, but the characteristic time scales differ by a factor of 50 at all hydration levels. The slow dynamics has a time scale of ~500 ps at low λ and ~160 ps at high λ . The slow proton population has been identified with a long-lived hydronium moiety with the implication that the hydronium ion lifetime in hydrated Nafion is of the order of 1 ns, which is in contrast to the case in bulk water where the hydronium ion lifetime is ~1 ps.⁷ This supports a slow diffusion mechanism where the hydronium ion moves as a well-defined entity (vehicular transport) at all hydration levels in Nafion.

Proton transport and water diffusion in hydrated Nafion have also been examined by numerous molecular modeling studies^{8,9,12–17} and their findings have been recently summarized by Elliott and Paddison.¹⁸ Petersen and Voth¹² have found the vehicular and structural transport of protons to be of similar magnitude but strongly negatively correlated in their study of hydrated Nafion using a self-consistent multistate empirical valence bond (SCI-MS-EVB) method. They concluded that sulfonate ions act as proton traps and limit hydronium diffusion. A previous study¹³ using a statistical mechanical model had shown that proton mobility is highest in the central region of hydrated Nafion pores well-separated from sulfonate groups.

Urata et al.¹⁵ used a united-atom force field to study water dynamics in Nafion membrane for $\lambda = 2.8, 5.9, 13.3$, and 35.4. Their calculated water diffusion coefficients were smaller than experimental values. Their results showed that water molecules located 2–4 Å away from the nearest sulfonate group had a shorter residence time than those located 4–6 or 6–8 Å away at $\lambda = 13.3$ and 35.4, which is at odds with the findings of Paul and Paddison.¹³ Moreover, the residence time of water molecules beyond 6 Å was found to increase with increasing level of hydration, which is in disagreement with the trends seen in QENS experiments.^{5,7} These disagreements may have arisen from the limitations imposed by the use of united-atom force fields. Moreover, a recent work¹⁹ has discussed the need to rigorously define the mean residence time of molecules.

In the present work, we have systematically determined the mean residence time of water molecules as a function of Nafion membrane hydration level. The paper is organized as follows: in section 2, we discuss the details of the simulation including the calculation of mean residence time of water molecules; in section 3, we discuss the diffusion of water molecules and hydronium ions in light of experimental findings; in section 4, we summarize our findings.

2. Details of the Simulation

2.1. Simulation Cell and Force Field. We performed classical MD simulations of hydrated Nafion with all-atom force

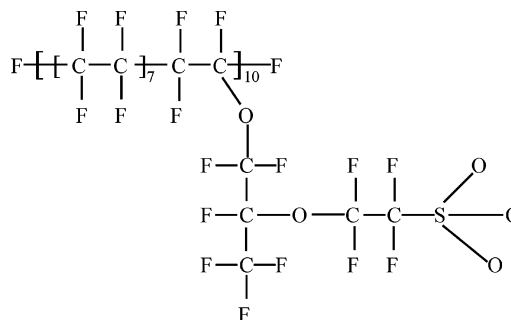


Figure 1. Chemical structure of Nafion.

fields. The chemical formula of a Nafion chain in the present work is shown in Figure 1. Each chain of Nafion has ten hydrophilic SO_3^- -terminated pendants spaced evenly by seven nonpolar $-\text{CF}_2-\text{CF}_2-$ monomers that form a hydrophobic backbone, referred to as a dispersed sequence by Jang et al.¹⁴ We assume all the sulfonate groups to be ionized based on the findings of Paddison and Elliott²⁰ for $\lambda \geq 3$. Four Nafion chains of 682 atoms each were contained in an orthorhombic simulation box with 40 H_3O^+ ions and from 0 to 760 H_2O molecules (H_2O wt % = 1.5–23.9) with periodic boundary conditions imposed. The simulated cells correspond to λ of 1, 3, 5, 7, 9, 11, 13.5, and 20, respectively. Since ab initio calculations²⁰ have shown that the proton is unlikely to transfer from the sulfonic acid group to water for $\lambda = 1$, this case was simulated mainly to establish a classical benchmark.

We performed all our simulations using the DL_POLY 2.16 code²¹ and the DREIDING force field^{14,22} for Nafion and F3C force field²³ for H_2O and H_3O^+ . The details of the implementation of these potentials such as cutoff distances have been discussed previously.⁸ Following energy minimization and annealing for each λ , which have been described in detail elsewhere,⁸ we equilibrated the system for 250 ps at 300 K using NPT MD simulation. The resulting system density varied from 1.76 g/cm³ for $\lambda = 1$ to 1.62 g/cm³ for $\lambda = 20$ and is in good agreement with corresponding experimental values.²⁴ Following equilibration, we performed NVT MD simulations at 300 K for 2 ns for each value of λ and saved the configurations at 0.2 ps intervals.

2.2. Diffusion Coefficients. We determined the diffusion coefficients, D , for the water oxygen (O_w) and hydronium oxygen (O_h) for various λ from the mean square displacement ($\text{MSD} = \langle |r(t) - r(0)|^2 \rangle$) as follows:

$$D = \frac{\langle |r(t) - r(0)|^2 \rangle}{6t} \quad (1)$$

We evaluated the MSD of O_w and O_h at 0.2 ps intervals and determined D over the time period from 1 to 2 ns.

2.3. Mean Residence Time. We have calculated mean residence times (τ_{MR}) of H_2O molecules and H_3O^+ ions in the first hydration shell around the SO_3^- groups to relate hydrated Nafion membrane nanostructure to dynamics of small molecules and ions. An approach commonly used in the literature is to define τ_{MR} of a molecule as the time span it stays in the solvation shell based on the idea of persisting coordination.^{25–27} To reduce problems that arise in the determination of τ_{MR} when a molecule makes frequent transits across the solvation shell boundary, excursions outside the solvation shell for a brief period, t^* , are allowed. The use of an arbitrarily chosen parameter, t^* , is considered a crude device to avoid elaborate bookkeeping²⁵ and its value has ranged from 0²⁷ to 2 ps.²⁵ Schröder et al.¹⁹ have

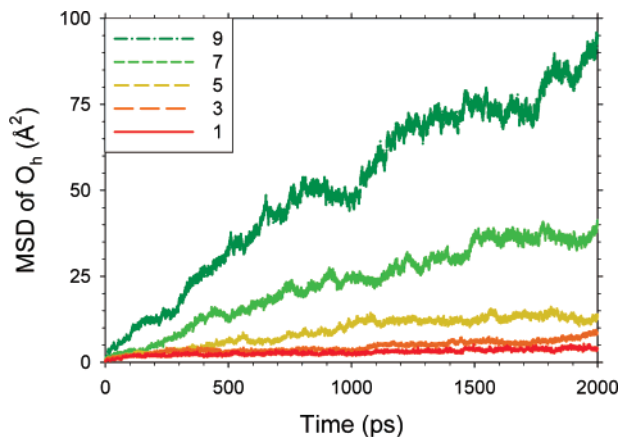


Figure 2. MSD of hydronium oxygen in Nafion at low hydration levels (λ) indicated by the legend.

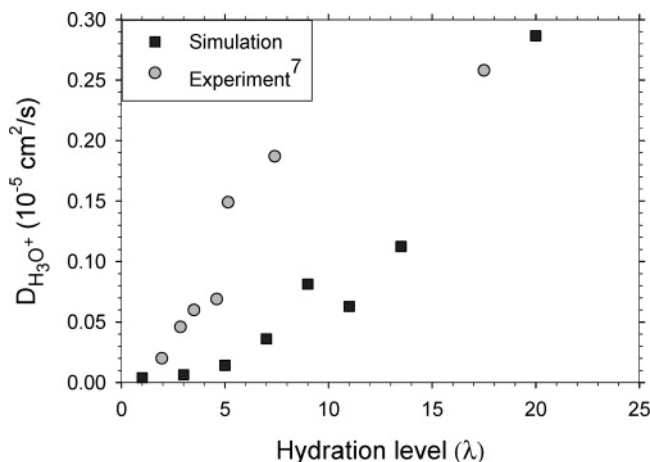


Figure 3. Diffusion coefficient of H_3O^+ ions at various hydration levels in Nafion from the present simulation (squares) and QENS experiment (circles).

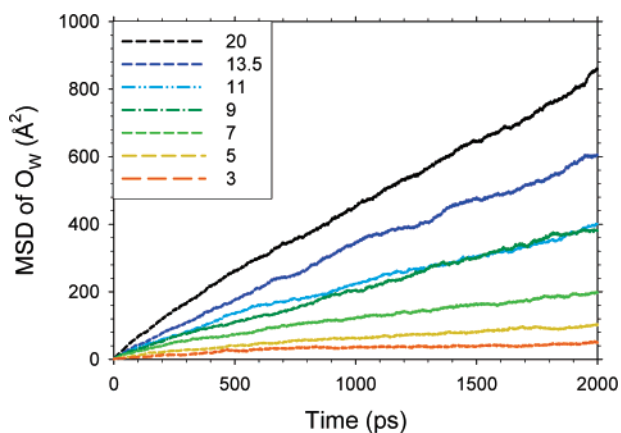


Figure 4. MSD of water oxygen in Nafion for hydration levels (λ) indicated by the legend.

argued that the above approach is unsatisfactory because it yields τ_{MR} values that are dependent on the radius of the solvation shell and the frequency of recorded trajectories.

Following the approach of Brunne et al.,²⁸ we have calculated τ_{MR} of H_2O molecules and H_3O^+ ions around a given SO_3^- group from 2000 configurations at 1 ps intervals. Consider a Boolean variable $v_i(t)$ that is 1 if the i th H_2O molecule is in the

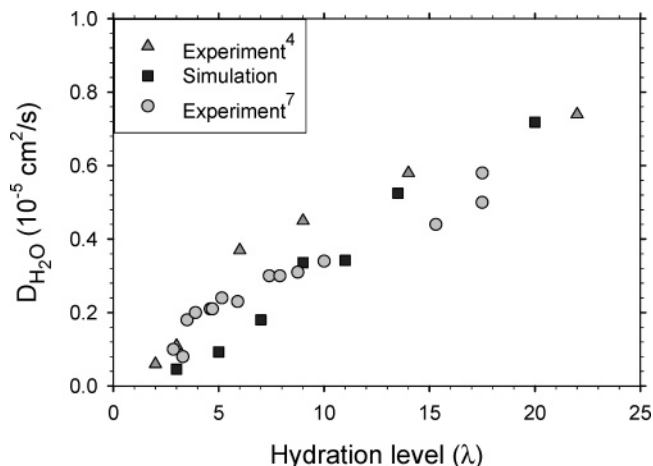


Figure 5. Variation of diffusion coefficient of H_2O molecules with hydration level in Nafion from the present simulation (squares), NMR experiment (triangles), and QENS experiment (circles).

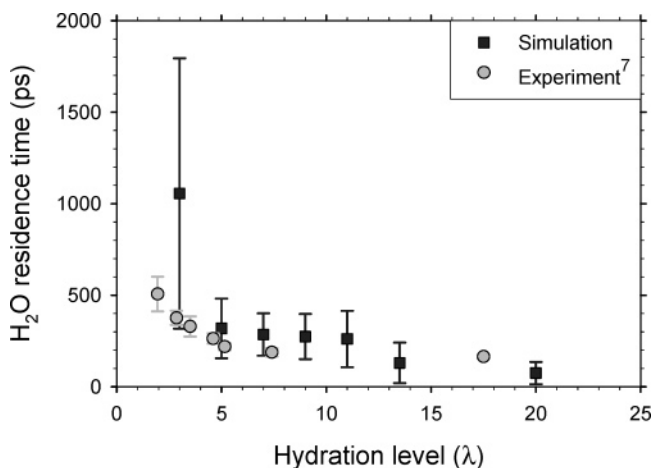


Figure 6. Variation of mean residence time (MRT) of H_2O molecules with hydration level in Nafion from the present simulation (squares) and MRT associated with slow dynamics observed in QENS experiment⁸ (circles).

solvation shell of a SO_3^- group at time t and 0 otherwise. The correlation function of this Boolean variable can be written as

$$f(t_k) = \sum_{j=1}^{M-k} \sum_{i=1}^N v_i(t_j) v_i(t_j + t_k) \quad (2)$$

$t_k = k\Delta t$ is the offset time, where $k = 0, 1, 2, \dots, 1800$ and $\Delta t = 1$ ps. The inner summation is over N H_2O molecules, while the outer summation is over $M-k$ time origins, t_j , such that $t_j = t_{j-1} + \Delta t$, $t_1 = 1$ ps, and $M = 2000$. The mean residence time, τ_{MR} , is obtained by fitting the correlation function to an exponential function, such that

$$f(t) = A \exp(-t/\tau_{\text{MR}}) \quad (3)$$

The same approach was used for H_3O^+ ions around a given SO_3^- group. The cutoff distance for the first solvation shell around a SO_3^- group was 4.3 Å for both H_2O molecules and H_3O^+ ions. This distance is consistent with our definition of bound water in the first part of this work.⁸

3. Results and Discussion

3.1. Diffusion Coefficients of H_3O^+ Ions and H_2O Molecules. Figure 2 shows the MSD of O_h as a function of time

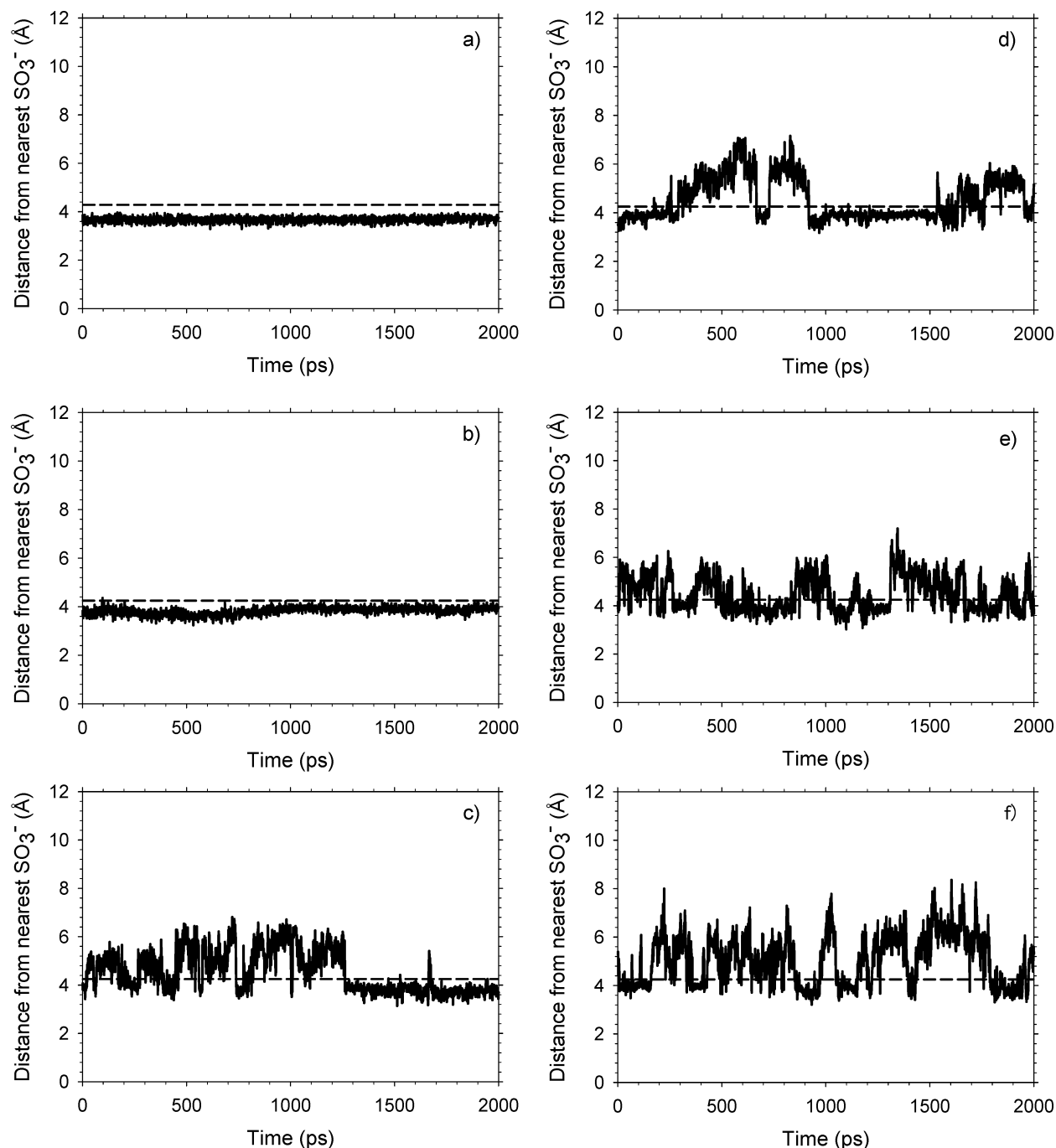


Figure 7. Distance from the nearest SO_3^- group for a H_3O^+ ion for λ values of (a) 1, (b) 3, (c) 5, (d) 7, (e) 9, and (f) 20. The horizontal line represents the radius of the first solvation shell.

for low hydration levels. We have plotted the data for λ values up to 9 to highlight the change in H_3O^+ ion dynamics around $\lambda = 5$. Our simulation reveals that there is a significant increase in the mobility of O_h for $\lambda = 7$ compared to that for $\lambda \leq 5$. We obtained the diffusion coefficient from the plot of MSD as a function of time according to eq 1 by averaging over 100 values sampled between 1 and 2 ns. Figure 3 shows the vehicular diffusion coefficient of the classical H_3O^+ ion from the present simulation at various hydration levels and the local diffusion coefficient of slow protons, identified as H_3O^+ ions, from QENS experiment.⁷ The hydration levels in the present study were chosen to cover the range of values examined by experiment,^{4–7} which facilitates validation of the simulation and interpretation of experimental results. The simulated values of $D_{\text{H}_3\text{O}^+}$ are smaller than the corresponding experimental values by a factor

of 2–5 except at $\lambda \sim 20$, where the agreement with experiment is good. This discrepancy reflects the limitation of classical models in probing hydronium dynamics. However, general trends in the experimental data are reproduced by the simulations. For instance, there is an abrupt increase in the diffusion of hydronium ions at $\lambda = 5$ as shown by experiment.⁷ This is related to changes in the hydration number and bridging configurations of H_3O^+ ions between SO_3^- groups observed in the first part of this work⁸ in agreement with the findings of a recent infrared spectroscopy experiment.⁶ Our simulated values of $D_{\text{H}_3\text{O}^+}$ show a rapid increase with increasing λ for $\lambda > 5$. The presence of multiple SO_3^- groups around the H_3O^+ ion at low hydration levels impedes the vehicular transport of the H_3O^+ ion. With increasing λ , the average number of SO_3^- groups around the H_3O^+ ion decreases,⁸ which contributes to increasing

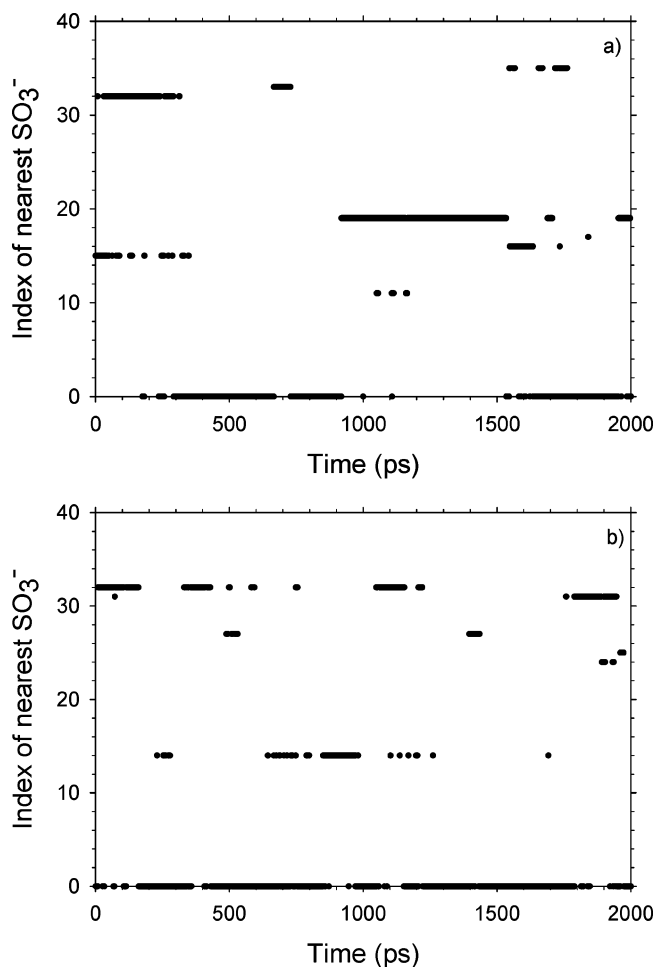


Figure 8. Index of the SO_3^- group that is nearest to a H_3O^+ ion for λ values of (a) 7 and (b) 20. An index of 0 indicates a free H_3O^+ ion.

vehicular diffusion of the H_3O^+ ion. Experimental studies have shown that the proton diffusion coefficient⁴ is comparable to $D_{\text{H}_3\text{O}^+}$ in hydrated Nafion at $\lambda = 3$, but is an order of magnitude higher at $\lambda \sim 20$. The first part of this study⁸ has shown that the hydration number of H_3O^+ ions increases with increasing λ from ~ 1.5 at $\lambda = 3$ to ~ 3.8 at $\lambda = 20$. This explains the increasing structural diffusion with increasing λ .

Figure 4 shows the MSD of O_w as a function of time for various hydration levels from $\lambda = 3$ to $\lambda = 20$. The data is in good agreement with the results of our earlier simulation of hydrated Nafion at 300 K using a different all-atom force field.⁹ Figure 5 shows the diffusion coefficient of H_2O molecules from the present simulation (squares) as a function of hydration level in Nafion. $D_{\text{H}_2\text{O}}$ increases with increasing λ and attains a value at $\lambda = 20$ that is one-third of the water diffusion coefficient in bulk water.²³ The experimental values of $D_{\text{H}_2\text{O}}$ obtained from NMR experiments⁴ and QENS study⁷ of water dynamics in hydrated Nafion are also shown as triangles and circles, respectively. Our simulation results are in good agreement with experimental data over a wide range of hydration levels, which attests to the ability of the all-atom force fields used in this work to model water dynamics in Nafion. In the first part of this work,⁸ we showed that the percentage of free (bulklike) water molecules increases from nearly 2.7% at $\lambda = 3$ to 66% at $\lambda = 20$, which is consistent with the increase of $D_{\text{H}_2\text{O}}$ with increasing λ . With increasing hydration level, water molecules are able to drift away from the SO_3^- groups into the water channels, which become increasingly interconnected.⁸

3.2. Mean Residence Time of H_2O Molecules and H_3O^+ Ions. We calculated τ_{MR} of H_2O molecules and H_3O^+ ions around each of the 40 SO_3^- groups belonging to four Nafion chains at each λ . Our simulations revealed the existence of a heterogeneous molecular environment in the simulation cell. Since the algorithm we used for calculating τ_{MR} is known to give longer residence times²⁹ than one based on persisting coordination^{25–27} and the simulation run was restricted to 2 ns due to computational intensity, some H_2O molecules or H_3O^+ ions were found to be bound to SO_3^- groups for the duration of the simulation resulting in $\tau_{\text{MR}} \rightarrow \infty$. This is consistent with the observation in the first part of this work⁸ that nearly a third of the water molecules are bound or weakly bound to the SO_3^- groups and $\sim 8\%$ of the H_3O^+ ions are coordinated by two or more SO_3^- groups at the highest hydration level simulated ($\lambda = 20$).

To overcome this difficulty arising from H_2O molecules or H_3O^+ ions being bound for the duration of the simulation, we determined τ_{MR} corresponding to each chain (averaged over 10 SO_3^- groups), instead of the whole simulation cell (40 SO_3^- groups), and report here the smallest of the four values of τ_{MR} at each λ . Figure 6 shows τ_{MR} of H_2O molecules in one chain of our hydrated Nafion system as a function of λ (squares) along with mean residence time corresponding to slow dynamics (τ_{slow}) observed in QENS experiments⁷ (circles). At $\lambda = 3$, τ_{MR} of H_2O molecules around a SO_3^- group is comparable to the total simulation time, which results in a large error bar. With increasing λ , τ_{MR} and τ_{slow} decrease and their values are comparable. τ_{MR} of H_2O molecules decreases from ~ 1055 ps at $\lambda = 3$ to ~ 75 ps at $\lambda = 20$. The experimental value⁷ of τ_{slow} ranges from 506 ps at $\lambda = 1.95$ to 165 ps at $\lambda = 17.5$.

We determined τ_{MR} of H_3O^+ ions only for $\lambda = 13.5$ and 20 and these were 572 ± 643 ps and 191 ± 214 ps, respectively. These values are 2.5–4.5 times larger than the corresponding values for H_2O molecules. At lower λ , each of the chains had at least one bound H_3O^+ ion for the duration of the simulation, which precluded the determination of τ_{MR} . Perrin et al.⁷ have offered three possible reasons for the characteristic time of slow protons (τ_{slow}) observed by QENS, namely, polymer chain dynamics, water clusters trapped in the polymer matrix, and hydronium ion dynamics. The present results are consistent with the third explanation; i.e., τ_{slow} is associated with the residence of H_3O^+ ions and H_2O molecules in the first solvation shell of SO_3^- groups in Nafion. Our results for τ_{MR} of H_3O^+ ions are also consistent with the observation of Perrin et al.⁷ that the H_3O^+ ion lifetime is of the order of or larger than 1 ns and the conclusion of Petersen and Voth¹² that sulfonate ions limit hydronium ion diffusion.

3.3. Distance of H_3O^+ Ions and H_2O Molecules from the Nearest SO_3^- Group. The mean residence time discussed in the previous section describes the average behavior of H_3O^+ ions and H_2O molecules. In an effort to shed more light on dynamical behavior in the vicinity of SO_3^- groups, we have determined the distance from the nearest SO_3^- group for individual H_3O^+ ions and H_2O molecules at 1 ps intervals during our 2 ns simulation. Figure 7a–f shows this distance for a randomly chosen H_3O^+ ion, for $\lambda = 1, 3, 5, 7, 9$, and 20, respectively. The distance reported here is between the oxygen of a H_3O^+ ion and the sulfur of its nearest SO_3^- group. It is clear from Figure 7a that the H_3O^+ ion is bound for the duration of the simulation at $\lambda = 1$ because the data fall entirely below the horizontal line representing the first solvation shell radius (4.3 Å) based on the S– O_h radial distribution function.⁸ At $\lambda = 3$ [see Figure 7b], the H_3O^+ ion is bound to the SO_3^- group

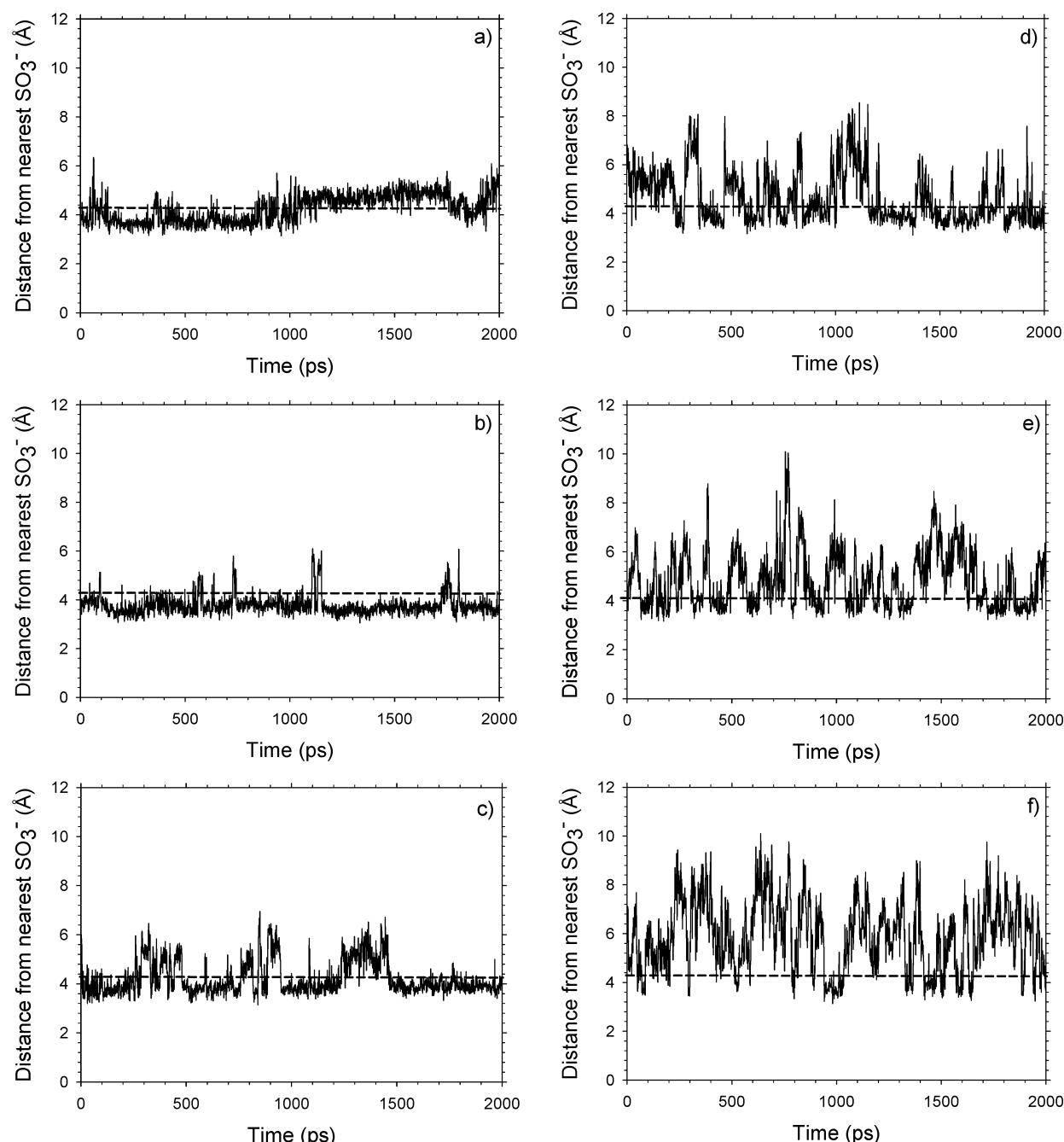


Figure 9. Distance from the nearest SO_3^- group to a H_2O molecule for values of (a) 3, (b) 5, (c) 7, (d) 9, (e) 13.5, and (f) 20. The horizontal line represents the radius of the first solvation shell.

but the distance approaches the radius of the first solvation shell. We have observed some H_3O^+ ions to remain close to the boundary of the solvation shell and transit frequently across this boundary for $\lambda = 3$. As λ increases from 5 to 9 [Figure 7c–e)], the average distance of the H_3O^+ ion from the nearest SO_3^- group increases. These hydration levels represent a transition from mostly bound (at lower λ) to mostly free H_3O^+ ion (at higher λ). While the variation of the distance to the nearest SO_3^- group is different for different H_3O^+ ions, the trend with increasing λ is similar and the average behavior is captured by τ_{MR} . At the highest hydration level, $\lambda = 20$, shown in Figure 7f, the H_3O^+ ion ventures as far as ~ 8 Å away from the nearest SO_3^- group and spends most of the simulation time as a free H_3O^+ ion. Even at this high hydration level, the H_3O^+ ion is bound to SO_3^- groups for a period of the order of 100 ps. Due to frequent transits of H_3O^+ ions across the solvation shell of

SO_3^- groups for $\lambda \geq 5$, it is possible to get much shorter mean residence times of the order of tens of picoseconds using an algorithm based on persistent coordination.^{25–27}

Figure 8a,b shows the index of the nearest SO_3^- group for the same H_3O^+ ion discussed above for hydration levels of 7 and 20, respectively. Indices of 1–10, 11–20, 21–30, and 31–40 represent the four chains, while an index of 0 indicates that no sulfur atom is present within 4.3 Å of the O_h (free H_3O^+). There is at most one SO_3^- nearest neighbor at a given time step, but the figure gives the appearance of multiple indices at a given time, because we have plotted 2000 data points that often lie close together. The H_3O^+ ion is coordinated by different SO_3^- groups belonging to different chains at various times during the course of the simulation, which indicates the H_3O^+ ion is able to move from one SO_3^- group to another even though its mean residence time is of the order of 1 ns. When viewed

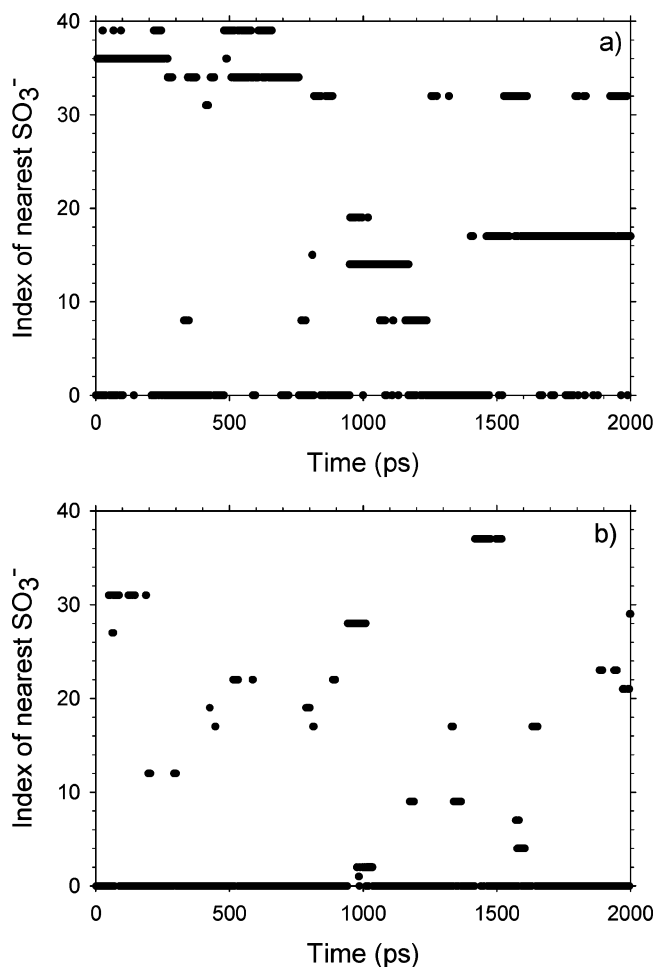


Figure 10. Index of the SO_3^- group that is nearest to a H_2O molecule for λ values of (a) 7 and (b) 20. An index of 0 indicates a free H_2O molecule.

together, Figures 7 and 8 provide valuable information about the path traveled by the H_3O^+ ion. The H_3O^+ ion spends some time bound to SO_3^- groups, moves away from the SO_3^- group toward the center of the Nafion nanopore, and subsequently becomes bound to a SO_3^- group that may be different from the one previously binding the H_3O^+ ion. The H_3O^+ ion residence time decreases and the frequency of the transit between SO_3^- groups increases as the hydration level increases. At low hydration level (say $\lambda = 7$), it is possible for the H_3O^+ ion to change its binding from one SO_3^- group to another without becoming free because there are several SO_3^- groups close to the H_3O^+ ion.

Figure 9a–f shows the distance between the oxygen of a randomly chosen H_2O molecule and the sulfur of the nearest SO_3^- group for $\lambda = 3, 5, 7, 9, 13.5$, and 20, respectively. The trends in the data are similar to that seen in Figure 7 for H_3O^+ ions. However, at a given λ , the H_2O molecule remains bound to the nearest SO_3^- group for a shorter time and travels farther from the SO_3^- group compared to H_3O^+ ions. At all hydration levels examined, the H_2O molecule spends some time being bound to the SO_3^- group, but this time decreases with increasing λ . Figure 10, parts (a) and (b), shows the index of the SO_3^- group nearest to the H_2O molecule represented in Figure 9, parts (c) and (f), corresponding to hydration levels of 7 and 20, respectively. As in the case of the H_3O^+ ion, the H_2O molecule is coordinated by different SO_3^- groups during the simulation. At $\lambda = 20$, the H_2O molecule is mostly free (index = 0), but binds for periods of the order of tens of picoseconds to SO_3^-

groups belonging to all four chains. At the highest hydration level examined [see Figure 9f], the H_2O molecule ventures ~ 10 Å from the nearest SO_3^- group.

We have found 11 Å to be the maximum S–O_h separation after examining the data for randomly chosen H_2O molecules at each λ . Gebel³⁰ has proposed a model of hydrated Nafion based on small-angle X-ray scattering that considers the dry membrane to be made of isolated spherical ionic clusters of radius ~ 7.5 Å that swell with increasing hydration. In this model, the hydrated membrane consists of pools of water of radius ~ 10 Å surrounded by ionic groups at the polymer–water interface.^{30,31} At high levels of hydration, water channels connect the spherical clusters. Our finding of a maximum separation of ~ 11 Å between a typical H_2O molecule and its nearest SO_3^- neighbor at $\lambda = 20$ is consistent with Gebel's model³⁰ of a spherical pool of water of radius 10 Å in hydrated Nafion.

The findings of this two-part work are as follows. At low hydration levels ($\lambda \leq 5$) in Nafion, H_3O^+ ions are coordinated by multiple SO_3^- groups and fewer than 20% of the H_2O molecules are free (bulklike). More than 50% of the hydronium ions exist in bridging configurations between sulfonate groups. As the hydration level increases, the sulfonate groups move apart and the hydration number of hydronium ions increases. The water molecules mediate the interaction between hydronium ions and sulfonate groups, leading to an increase in their separation distance. With increasing hydration level, the diffusion coefficients of H_3O^+ ions and H_2O molecules increase and the mean residence time of water molecules around sulfonate groups decreases.

The calculation of mean residence times of H_2O molecules and H_3O^+ ions in Nafion at various hydration levels by a rigorous method that avoids difficulties arising from frequent transit across the solvation shell boundary is an important contribution of this work. The long residence times (~ 1 ns) of H_2O molecules and H_3O^+ ions indicates that longer scale simulations may be needed to understand dynamical behavior at low hydration levels. Our results provide a molecular-level explanation for the conclusion of Kreuer et al.¹⁰ and Zawodzinski et al.⁴ that vehicular proton transport is dominant at low hydration levels while structural diffusion dominates proton transport at high hydration levels in Nafion.

4. Conclusions

We have calculated the diffusion coefficients of water molecules in Nafion at various hydration levels and found them to be in good agreement with experimental data. At high hydration levels, the calculated diffusion coefficient of hydronium ions is in agreement with the value reported by a recent QENS experiment. Our simulations reveal that H_2O molecules and H_3O^+ ions migrate by diffusion between the solvation shell of different SO_3^- groups and the center of the Nafion pore. The mean residence time of H_2O molecules near sulfonate groups decreases with increasing hydration level from ~ 1 ns at $\lambda = 5$ to ~ 75 ps at $\lambda = 20$. The mean residence time of H_3O^+ ions is larger than the corresponding values for H_2O molecules by a factor of 2.5–4.5. Our work provides an explanation for the experimentally observed characteristic time of slow proton dynamics in hydrated Nafion in terms of the residence of H_3O^+ ions and H_2O molecules in the first solvation shell of SO_3^- groups. The present results in conjunction with the results from the first part of this work establish an important link between Nafion membrane nanostructure and the dynamics of H_2O molecules and H_3O^+ ions.

Acknowledgment. This work was supported by the U.S. Department of Energy's (DOE) Office of Basic Energy Sciences, Chemical Sciences program, and was performed in part using the Molecular Science Computing Facility (MSCF) in the William R. Wiley Environmental Molecular Sciences Laboratory, a DOE national scientific user facility located at the Pacific Northwest National Laboratory (PNNL). PNNL is operated by Battelle for DOE. This work benefited from resources of the National Energy Research Scientific Computing Center, which is supported by the Office of Science of the U.S. Department of Energy under Contract No. DE-AC03-76SF00098.

References and Notes

- (1) Crabtree, G. W.; Dresselhaus, M. S.; Buchanan, M. V. *Phys. Today* **2004**, 57 (12), 39.
- (2) Eikerling, M.; Kornyshev, A. A.; Kucernak, A. R. *Phys. Today* **2006**, 59 (10), 38.
- (3) Paciaroni, A.; Casciola, M.; Cornicchi, E.; Marconi, M.; Onori, G.; Pica, M.; Narducci, R. *J. Phys. Chem. B* **2006**, 110, 13769.
- (4) Zawodzinski, T. A.; Neeman, M.; Sillerud, L. O.; Gottesfeld, S. *J. Phys. Chem.* **1991**, 95, 6040.
- (5) Pivovar, A. M.; Pivovar, B. S. *J. Phys. Chem. B* **2005**, 109, 785.
- (6) Moilanen, D. E.; Piletic, I. R.; Fayer, M. D. *J. Phys. Chem. A* **2006**, 110, 9084.
- (7) Perrin, J.-C.; Lyonnard, S.; Volino, F. *J. Phys. Chem. C* **2007**, 111, 3393.
- (8) Devanathan, R.; Venkatnathan, A.; Dupuis, M. *J. Phys. Chem. B* **2007**, 111, 8069.
- (9) Venkatnathan, A.; Devanathan, R.; Dupuis, M. *J. Phys. Chem. B* **2007**, 111, 7234.
- (10) Kreuer, K.-D.; Paddison, S. J.; Spohr, E.; Schuster, M. *Chem. Rev.* **2004**, 104, 4637.
- (11) Marx, D.; Tuckerman, M. E.; Hutter, J.; Parrinello, M. *Nature* **1999**, 397, 601.
- (12) Petersen, M. K.; Voth, G. A. *J. Phys. Chem. B* **2006**, 110, 18594.
- (13) Paul, R.; Paddison, S. *J. Chem. Phys.* **2005**, 123, 224704.
- (14) Jang, S. S.; Molinero, V.; Çağın, T.; Goddard, W. A. *J. Phys. Chem. B* **2004**, 108, 3149.
- (15) Urata, S.; Irisawa, J.; Takada, A.; Shinoda, W.; Tsuzuki, S.; Mikami, M. *J. Phys. Chem. B* **2005**, 109, 4269.
- (16) Cui, S.; Liu, J.; Selvan, M. E.; Keffer, D. J.; Edwards, B. J.; Steele, W. V. *J. Phys. Chem. B* **2007**, 111, 2208.
- (17) Blake, N. P.; Mills, G.; Metiu, H. *J. Phys. Chem. B* **2007**, 111, 2490.
- (18) Elliott, J. A.; Paddison, S. J. *J. Phys. Chem. Chem. Phys.* **2007**, 9, 2602.
- (19) Schröder, C.; Rudas, T.; Boresch, S.; Steinhäuser, O. *J. Chem. Phys.* **2006**, 124, 234907.
- (20) Paddison, S. J.; Elliott, J. A. *J. Phys. Chem. A* **2005**, 109, 7583.
- (21) Smith, W.; Forester, T. R. *J. Mol. Graphics* **1996**, 14, 136.
- (22) Mayo, S. L.; Olafson, B. D.; Goddard, W. A. *J. Phys. Chem.* **1990**, 94, 8897.
- (23) Levitt, M.; Hirshberg, M.; Sharon, R.; Laidig, K. E.; Daggett, V. *J. Phys. Chem. B* **1997**, 101, 5051.
- (24) Morris, D. R.; Sun, X. *J. Appl. Polym. Sci.* **1993**, 50, 1445.
- (25) Impey, R. W.; Madden, P. A.; McDonald, I. R. *J. Phys. Chem.* **1983**, 87, 5071.
- (26) Luise, A.; Falconi, M.; Desideri, A. *Proteins: Struct. Funct. Genet.* **2000**, 39, 56.
- (27) Garcia, A. E.; Stiller, L. *J. Comput. Chem.* **1993**, 14, 1396.
- (28) Brunne, R. M.; Liepinsh, E.; Otting, G.; Wüthrich, K.; van Gunsteren, W. F. *J. Mol. Biol.* **1993**, 231, 1040.
- (29) Schoenborn, B. P.; Garcia, A.; Knott, R. *Prog. Biophys. Mol. Biol.* **1995**, 64, 105.
- (30) Gebel, G. *Polymer* **2000**, 41, 5829.
- (31) Mauritz, K. A.; Moore, R. B. *Chem. Rev.* **2004**, 104, 4535.